

Ground state and excitation dynamics in Ag doped helium clusters

Massimo Mella*

*Dipartimento di Chimica Fisica ed Elettrochimica,
Università degli Studi di Milano, via Golgi 19, 20133 Milano, Italy*

Maria Carola Colombo[†] and Gabriele Morosi[†]

*Dipartimento di Scienze Chimiche, Fisiche e Matematiche,
Università dell'Insubria, via Lucini 3, 22100 Como, Italy*

We present a quantum Monte Carlo study of the structure and energetics of silver doped helium clusters AgHe_n for n up to 100. Our simulations show the first solvation shell of the Ag atom to be composed by roughly 20 He atoms, and to possess a structured angular distribution. Moreover, the electronic $^2\text{P}_{1/2} \leftarrow ^2\text{S}_{1/2}$ and $^2\text{P}_{3/2} \leftarrow ^2\text{S}_{1/2}$ electronic transitions of the embedded silver impurity have been studied as a function of the number of helium atoms. The computed spectra show a redshift for $n \leq 15$ and an increasing blueshift for larger clusters, a feature attributed to the effect of the second solvation shell of He atoms. For the largest cluster, the computed excitation spectrum is found in excellent agreement with the ones recorded in superfluid He clusters and bulk. No signature of the direct formation of proposed AgHe_2 exciplex is present in the computed spectra of AgHe_{100} .

PACS numbers:

Superfluid ^4He clusters represent a gentle environment where high resolution spectroscopic studies of atoms, atomic clusters, and molecules at low temperature can be carried out [1]. In such cold and fluid quantum systems many perturbing effects due to the temperature and solid matrices are absent, allowing therefore for an easier interpretation of the experimentally recorded spectra. Moreover, their superfluid behavior allows interesting quantum effects to take place and to be experimentally probed (for instance see Refs. [2, 3]).

Whereas the coupling of the rotational and vibrational motion of the molecules with the quantum motion of the solvent is permitted by the similarity between energy levels, the electronic structure of an atom is characterized by energy differences orders of magnitude larger than the ones needed to induce excitation in the atomic motion. Although this difference might seem to work in the direction of simplifying the physical description of the electronic transition processes, many important details still wait to be clarified. As an example, the fluorescent D_2 emission line (i.e. the $^2\text{S}_{1/2} \leftarrow ^2\text{P}_{3/2}$ radiative transition) of heavy single valence electron atoms dispersed in superfluid helium is absent, while the D_1 line is sharp and only slightly shifted (1-2 nm) to the blue [4]. This is in contrast with the large broadening and strong blueshift of the absorption lines. Moreover, some features of the LIF spectra of the dispersed Ag were interpreted as signature of the AgHe and AgHe_2 exciplex formation [5].

The blueshift and broadening of the absorption lines

have been interpreted by means of a "bubble model". Here, the dispersed atom is enclosed in a spherical cavity due to the exchange repulsion of its valence electrons and the He ones. The liquid He around an atom is modeled by an isotropic sharp-edge density profile with no atomic internal structure. However, both the simple spherical bubble model [6] and the one where quadrupolar distortions of the spherical cavity are allowed [7] neither quantitatively predict the absorption spectrum of Cs and Rb, nor allow to interpret the small splitting of the Rb D_2 line. Reasonably, the lack of any shell structure in the helium density profile, the absence of a full atomistic description during the excitation process, and the physically incomplete description of the bubble distortion by means of simple quadrupolar deformations may be held responsible for this undesired outcome [8].

In order to gain a better understanding of the excitation process and its dependency on the degree of "solvation" of the impurity, we feel a direct many-body simulation of the excitation spectra to be mandatory. This also allows to explore the change in the spectra upon the increase of the number of He atoms in the clusters, and, at the same time, to test the validity of our theoretical approach.

With these goals in mind, we present a diffusion Monte Carlo study of the $^2\text{P}_{3/2} \leftarrow ^2\text{S}_{1/2}$ and $^2\text{P}_{1/2} \leftarrow ^2\text{S}_{1/2}$ absorption spectra of silver doped helium clusters. The Ag spectrum, both in bulk helium and in He clusters, has been deeply studied and well characterized [5, 9, 10] showing that Ag is indeed solvated. Moreover, accurate interaction potentials between He and the excited $^2\text{S}_{1/2}$, $^2\text{P}_{1/2}$, and $^2\text{P}_{3/2}$ states of Ag are available [11]. These potentials allowed to assign the broad band at 382 nm in the fluorescence spectrum to the AgHe_2 exciplex [5].

To tackle the atomic description needed to compute the excitation spectra, we believe the Monte Carlo meth-

*Electronic address: Massimo.Mella@unimi.it

[†]Present address: Laboratory of Inorganic Chemistry, ETH Hönggerberg, CH-8093 Zürich, Switzerland; Electronic address: Colombo@inorg.chem.ethz.ch

[‡]Electronic address: Gabriele.Morosi@uninsubria.it

ods are the best suited techniques. Since these methods are well described in the literature [12], we simply state that while variational Monte Carlo (VMC) allows one to optimize a trial wave function $\Psi_T(\mathbf{R})$ and to successively compute any expectation values $\langle O \rangle_{VMC}$ from it, diffusion Monte Carlo (DMC) corrects the remaining deficiencies of the variational description projecting out all the excited state components sampling $f(\mathbf{R}) = \Psi_0(\mathbf{R})\Psi_T(\mathbf{R})$, or less commonly $f(\mathbf{R}) = \Psi_0^2(\mathbf{R})$.

In atomic units, the Hamiltonian operator for our AgHe_n clusters reads as

$$\mathcal{H} = -\frac{1}{2} \left(\sum_{i=1}^n \frac{\nabla_i^2}{m_{^4\text{He}}} + \frac{\nabla_{\text{Ag}}^2}{m_{\text{Ag}}} \right) + V(\mathbf{R}) \quad (1)$$

Here, we assume a pair potential of the form $V(\mathbf{R}) = \sum_{i < j} V_{\text{HeHe}}(r_{ij}) + \sum_i V_{\text{AgHe}}(r_i)$ for the clusters with the silver atom in the ${}^2\text{S}_{1/2}$ electronic ground state. For $V_{\text{HeHe}}(r_{ij})$ we employed the TTY potential [13], and for $V_{\text{AgHe}}(r_i)$ we fitted the ${}^2\Sigma$ AgHe potential by Jakubek and Takami [11]. We computed the energy of the AgHe dimer by means of a grid method [14] obtaining -4.021 cm^{-1} : this value differs from their result (-4.000 cm^{-1}) by only 0.021 cm^{-1} .

Our trial wave function has the common form $\Psi_T(\mathbf{R}) = \prod_{i < j}^N \psi(r_{ij}) \prod_i^N \phi(r_i)$, where no one-body part was used, and $\psi(r) = \phi(r) = \exp[-\frac{p_5}{r^5} - \frac{p_3}{r^3} - \frac{p_2}{r^2} - p_1 r - p_0 \ln(r)] + a \exp[-b(r - r_0)^2]$. The parameters of the model wave function were fully optimized minimizing the variance of the local energy for each cluster. The sampled distributions were used to compute exactly the energy using the mixed estimator

$$\langle \mathcal{H} \rangle_M = \frac{\int f(\mathbf{R}) \mathcal{H}_{loc}(\mathbf{R}) d\mathbf{R}}{\int f(\mathbf{R}) d\mathbf{R}} \quad (2)$$

as well as the mixed and second order estimate $\langle \mathcal{O} \rangle_{SOE} = 2\langle \mathcal{O} \rangle_M - \langle \mathcal{O} \rangle_{VMC}$ of many other expectation values (e.g. the interparticle distribution functions) [12].

The resulting DMC energy values for the AgHe_n clusters with n up to 100 are shown in Table I together with the differential quantity $\Delta(n) = -[E(n) - E(m)]/(n - m)$, which can be interpreted as the evaporation energy of an He atom from the cluster. AgHe_m is the largest cluster having $m < n$.

From this data it can be noticed that $\Delta(n)$ does not possess a monotonic behavior. Instead, the steady increase for $n < 13$ is followed by a rapid decrease in value before plateauing for $n \sim 25$. This behavior could be interpreted invoking different effects. For $n < 13$, a newly added helium feels the bare Ag interaction potential plus the interaction with the already present He atoms, that acts positively increasing the binding energy. Quantitatively, we found the changes of $\Delta(n)$ versus n similar to the ones obtained for He_n [15], He_nH^- [16], and He_nHF [17]. Since this effect seems to be independent of the nature of the doping impurity, one may interpret it as a dynamical many-body effect of the interacting helium atoms.

n	$E(n)$	$\Delta(n)$	D_1	D_2
free Ag			338.3	328.1
1	-4.0212(9)			
2	-8.2333(5)	4.212(1)	344.5	334.8
3	-12.598(2)	4.365(2)	344.2	334.6
4	-17.112(1)	4.514(2)		
6	-26.478(2)	4.682(2)	342.6	333.3
8	-36.259(4)	4.890(2)	341.3	332.3
12	-56.68(1)		339.6	329.8
13	-61.78(1)	5.09(1)		
14	-66.84(1)	5.06(2)		
15	-71.61(5)	4.77(6)	338.3	328.5
19	-89.31(2)			
20	-93.17(3)	3.86(4)	337.3	327.6
24	-107.14(4)	3.49(1)		
25	-110.3(1)	3.2(1)		
29	-123.17(7)			
30	-126.11(7)	3.0(1)	336.2	326.6
40	-158.70(6)	3.26(1)	335.5	325.7
50	-191.3(3)	3.27(3)	334.7	324.9
60	-225.1(2)	3.38(4)	333.8	323.9
70	-259.9(4)	3.47(5)	333.4	323.6
80	-292.4(7)	3.26(8)	332.5	322.7
90	-326.2(7)	3.38(9)	331.9	322.0
100	-357.3(6)	3.10(9)	331.6	321.7

TABLE I: Total and evaporation energy (cm^{-1}), D_1 and D_2 absorption wavelengths (nm) for AgHe_n clusters.

Beyond AgHe_{13} , the value of $\Delta(n)$ decreases indicating the onset of a repulsive interaction. This could be attributed to an "excluded volume" effect, where each new He is strongly attracted by Ag in its first coordination shell, but has to "find room" for itself forcing the other atoms to increase their local density, and rising their average kinetic energy.

Finally, for clusters larger than AgHe_{25} , the evaporation energy remains roughly constant around $3.1\text{--}3.5 \text{ cm}^{-1}$ indicating that a new He atom feels a quite different environment than for $n < 25$.

Figure 1 represents the interparticle Ag-He probability density functions for clusters having n from 12 to 100. These were normalized so that $4\pi \int_0^\infty r^2 \rho(r) dr = n$, therefore representing the local density of He atoms around Ag. The functions for $n < 12$ overlap in shape with the AgHe_{12} one. As to AgHe_{30} , the presence of a broad shoulder at large r , that successively develops into a well defined peak, unambiguously indicates a second shell. More interestingly, the height of the first peak continuously rises until the second shell is completely filled, as indicated by the onset of another shoulder at large Ag-He distance for AgHe_{100} . Moreover, the density minimum between the first and second shell peaks also increases in height on going towards larger clusters, becoming just 15% less than the second shell peak height. Both these evidences can be interpreted as a direct signature of the "non rigidity" of the first He layer, as well as of an easy exchange process between the first and second

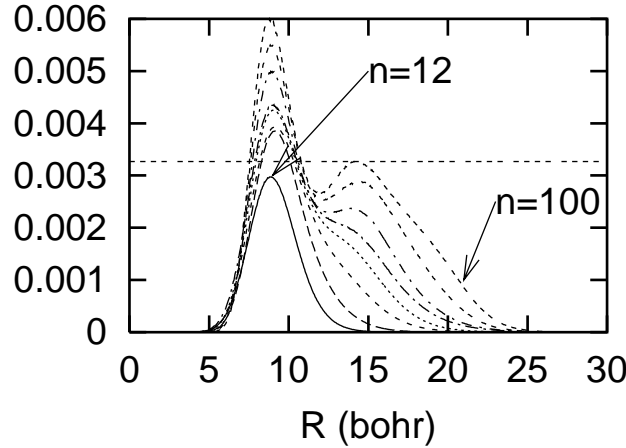


FIG. 1: He density distributions around Ag for $n = 12, 20, 30, 40, 50, 60, 80$, and 100 .

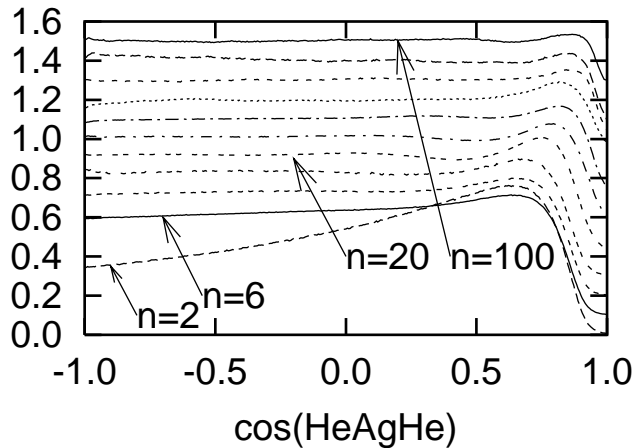


FIG. 2: $\cos(\text{HeAgHe})$ density distributions for $n = 2, 6, 8, 12, 20, 30, 40, 50, 60, 80$, and 100 . Each distribution is shifted upwards with respect to the previous one by 0.1.

shell [18].

As to the angular distributions, Figure 2 shows several $\cos(\text{HeAgHe})$ distributions. The smaller clusters ($n \leq 20$) show a deep minimum for $\cos(\text{HeAgHe}) = 1$ and a smooth maximum located in the 0.6-0.8 range, both strong indications of a structured distribution of the He atoms in the first solvation shell. Here, the minimum indicates that two He atoms cannot overlap or surmount each other, the only two possible arrangements having $\cos(\text{HeAgHe}) = 1$. Whereas the overlap is forbidden by the repulsive part of the He-He potential, the possibility of an He atom to surmount another is hindered by the strength of the $^2\Sigma$ AgHe potential that forces the He motion in a limited radial region around Ag as shown by the AgHe_{12} radial distribution. Instead, the smooth maximum indicates the relative localization effects due to the attractive interaction between He atoms.

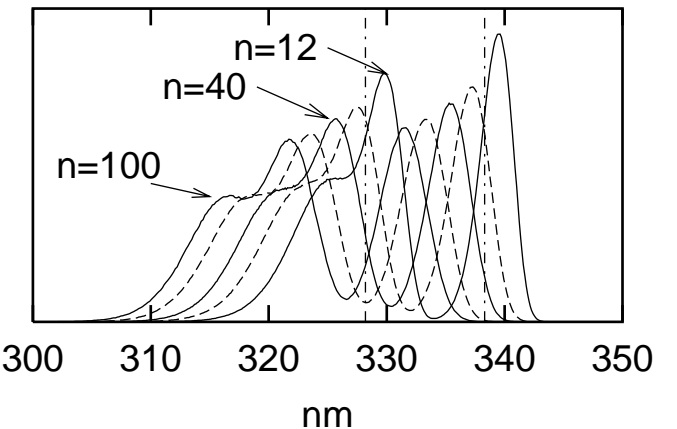


FIG. 3: Simulated absorption spectra for AgHe_n clusters with $n = 12, 20, 40, 70$, and 100 . The vertical lines represent the free Ag spectrum.

This effect is particularly evident for AgHe_2 , whose angular distribution function decreases on going towards $\cos(\text{HeAgHe}) = -1$. The position of the maximum shifts to larger $\cos(\text{HeAgHe})$ values on going from $n = 2$ to $n = 20$, suggesting a progressively more structured packing of the He atoms in the first shell for $n = 20$, and agreeing nicely with the aforementioned "excluded volume" interpretation. The structured packing is also supported by the shallow second peak located around 0.1 in the AgHe_{20} cosine distribution. Both the minimum and the maximum are "smeared out" by adding He atoms to AgHe_{20} , a clear indication that the second shell is less structured and more fluid than the first one.

As to the absorption spectrum of the embedded Ag atom, we computed this observable using the semiclassical approach proposed by Lax [19], and adapted to the quantum Monte Carlo framework by Cheng and Whaley [20]. In this method, the spectral lines are computed collecting the distribution of the difference $V_{\text{exc}}(\mathbf{R}) - V_{\text{gs}}(\mathbf{R})$ or, more accurately, of the quantity $V_{\text{exc}}(\mathbf{R}) + \sum_{i < j} V_{\text{HeHe}}(r_{ij}) - E_0$ over the sampled $f(\mathbf{R})$ [21]. Here, $V_{\text{gs}}(\mathbf{R})$ ($V_{\text{exc}}(\mathbf{R})$) is the interaction potential between the ground (excited) state Ag atom with the surrounding He atoms, while E_0 is the DMC ground state energy. The three $V_{\text{exc}}(\mathbf{R})$ PES for a given cluster configuration are obtained from the AgHe $^2\Pi_{1/2}$, $^2\Pi_{3/2}$, and $^2\Sigma$ interaction potentials using the Diatomic-in-Molecules approach. The details are well described by Nakayama and Yamashita for the Li, Na, and K cases [22].

The spectra obtained collecting $V_{\text{exc}}(\mathbf{R}) - V_{\text{gs}}(\mathbf{R})$ during the simulations are shown in Table I, and in Figure 3 for several representative clusters. The same quantities obtained by collecting $V_{\text{exc}}(\mathbf{R}) + \sum_{i < j} V_{\text{HeHe}}(r_{ij}) - E_0$ are blueshifted by less than 1 nm. The computed spectra clearly show the two separated bands deriving from

the excitation of Ag into $^2P_{1/2}$ and $^2P_{3/2}$ states, the second one also displaying the classical short wavelength shoulder typical of the D₂ line of heavy alkali atoms in superfluid helium [6, 7]. For our largest cluster, the D₁ and D₂ lines have maxima located at 331.6 and 321.7 nm, and a FWHM of 4.3 and 9.8 nm, respectively. These results are in accurate agreement with the experimental wavelengths 332.8 and 322.5 nm, and FWHM 4.0 and 8.5 nm [10].

From the spectra shown in Fig. 3, it clearly appears that the broadening of the absorption bands increases on going towards larger clusters. This evidence indicates that the Ag electronic degrees of freedom are coupled with the motion of an increasing number of He atoms, and not only with those located in the first shell. More interestingly, whereas all the clusters with $n \leq 15$ show a redshift with respect to the free Ag lines, the ones with $n \geq 19$ display a blueshift strongly dependent on the number of He atoms. Here, the redshift for $n \leq 15$ indicates that the clusters possess an internal distribution such that a vertical transition brings them in a region of the excited state potential where the complexes can form a bound state. This may give the possibility of producing AgHe _{n} ($n = 1-15$) exciplexes starting from the corresponding clusters, and to experimentally study their spectrum and decaying dynamics. Conversely, the larger clusters are vertically excited to repulsive regions of the potential energy surface (PES), therefore preventing the direct formation of larger exciplexes.

The blueshift for $n \geq 19$, at variance with basic solvation concepts, indicates a large effect of the second shell filling on the absorption wavelengths. This is confirmed by the computational evidence that the excitation spectrum of AgHe₁₀₀, that shows the onset of a third shell, closely agrees with the one of AgHe₉₀ (see Table I).

In order to rationalize this observation, as well as the monotonic blueshift of the absorption bands upon increasing of n , one must notice that the portion of the AgHe pair distribution located in the 10-13 bohr range overlaps with the tail of the repulsive excited AgHe $^2\Sigma$ potential. As a consequence, this zone of the pair density introduces some positive contribution to the diagonal elements of the matrix whose eigenvalues define the three electronic excited PES of the complexes. Since the magnitude of these contributions is dependent on the local He density via the sum $\sum V_{2\Sigma}(r)$ over the He atoms falling in that range, there is a net increase of the values of the diagonal elements upon increasing of the size of the cluster. This fact reflects itself in a positive shift of the eigenvalues, and hence in the blueshift of the computed spectra.

The authors thank Prof. Michio Takami for sending the computed interaction potentials. This work was supported by Italian MIUR Grant No. MM03265212. The authors are indebted to the Centro CNR per lo Studio delle Relazioni tra Struttura e Reattività Chimica for grants of computer time.

[1] J. P. Toennies and A. F. Vilesov, *Annu. Rev. Phys. Chem.* **49**, 1 (1998).

[2] K. Nauta and R. E. Miller, *Science* **287**, 293 (2000); *ibid* **283**, 1895 (1999).

[3] Y. Kwon, P. Huang, M. V. Patel, D. Blume, and K. B. Whaley, *J. Chem. Phys.* **113**, 6469 (2000).

[4] Y. Takahashi, K. Sano, T. Kinoshita, and T. Yabuzaki, *Phys. Rev. Lett.* **71**, 1035 (1993).

[5] J. L. Persson, Q. Hui, Z. J. Jakubek, M. Nakamura, and M. Takami, *Phys. Rev. Lett.* **76**, 1501 (1996).

[6] T. Kinoshita, K. Fukuda, Y. Takahashi, and T. Yabuzaki, *Phys. Rev. A* **52**, 2707 (1995).

[7] T. Kinoshita, K. Fukuda, and T. Yabuzaki, *Phys. Rev. B* **54**, 6600 (1996).

[8] S. Ogata, *J. Phys. Soc. Japan* **68**, 2153 (1999).

[9] Z. J. Jakubek, Q. Hui, and M. Takami, *Phys. Rev. Lett.* **79**, 629 (1997).

[10] A. Bartelt, J. D. Close, F. Federmann, N. Quaas, and J. P. Toennies, *Phys. Rev. Lett.* **77**, 3525 (1996).

[11] Z. J. Jakubek and M. Takami, *Chem. Phys. Lett.* **265**, 653 (1997).

[12] B. L. Hammond, W. A. Lester, Jr., and P. J. Reynolds, *Monte Carlo Methods in Ab Initio Quantum Chemistry*, 1st ed., (World Scientific, Singapore, 1994).

[13] K. T. Tang, J. P. Toennies, and C. L. Yiu, *Phys. Rev. Lett.* **74**, 1546 (1995).

[14] F. L. Tobin and J. Hinze, *J. Chem. Phys.* **63**, 1034 (1975).

[15] M. Lewerenz, *J. Chem. Phys.* **106**, 4596 (1997).

[16] M. Casalegno, M. Mella, G. Morosi, and D. Bressanini, *J. Chem. Phys.* **112**, 69 (2000).

[17] D. Blume, M. Lewerenz, F. Huisken, and M. Kaloudis, *J. Chem. Phys.* **105**, 8666 (1996).

[18] M. Buzzacchi, D. E. Galli, and L. Reatto, *Phys. Rev. B* **64**, 094512 (2001).

[19] M. Lax, *J. Chem. Phys.* **20**, 1752 (1952).

[20] E. Cheng and K. B. Whaley, *J. Chem. Phys.* **104**, 3155 (1996).

[21] While Cheng and Whaley [20] were forced to approximately estimate the contribution from the kinetic energy of the doping impurity to the computed solid matrix spectra, for finite systems as our clusters this can be exactly accounted for simply using the total ground state energy.

[22] A. Nakayama and K. Yamashita, *J. Chem. Phys.* **114**, 780 (2001).